HHS Public Access

Author manuscript

J Med Eng Technol. Author manuscript; available in PMC 2020 March 03.

Published in final edited form as:

J Med Eng Technol. 2018 February ; 42(2): 128–139. doi:10.1080/03091902.2018.1435745.

Spinal dura mater: biophysical characteristics relevant to medical device development

Sean J. Nagel[a], **Chandan G. Reddy**[b], **Leonardo A. Frizon**[a], **Matthieu K. Chardon**[c], **Marshall Holland**[b], **Andre G. Machado**[a], **George T. Gillies**[d], **Matthew A. Howard III**[b], **Saul Wilson**[b]

[a]Center for Neurological Restoration, Cleveland Clinic, Cleveland, OH, USA;

[b]Department of Neurosurgery, University of Iowa Hospitals and Clinics, Iowa City, IA, USA;

[c]Department of Physiology, Northwestern University Feinberg School of Medicine, Chicago, IL, USA;

[d]Department of Mechanical and Aerospace Engineering, University of Virginia, Charlottesville, VA, USA

Abstract

Understanding the relevant biophysical properties of the spinal dura mater is essential to the design of medical devices that will directly interact with this membrane or influence the contents of the intradural space. We searched the literature and reviewed the pertinent characteristics for the design, construction, testing, and imaging of novel devices intended to perforate, integrate, adhere or reside within or outside of the spinal dura mater. The spinal dura mater is a thin tubular membrane composed of collagen and elastin fibres that varies in circumference along its length. Its mechanical properties have been well-described, with the longitudinal tensile strength exceeding the transverse strength. Data on the bioelectric, biomagnetic, optical and thermal characteristics of the spinal dura are limited and sometimes taken to be similar to those of water. While various modalities are available to visualise the spinal dura, magnetic resonance remains the best modality to segment its structure. The reaction of the spinal dura to imposition of a foreign body or other manipulations of it may compromise its biomechanical and immune-protective benefits. Therefore, dural sealants and replacements are of particular clinical, research and commercial interest. In conclusion, existing devices that are in clinical use for spinal cord stimulation, intrathecal access or intradural implantation largely adhere to traditional designs and their attendant limitations. However, if future devices are built with an understanding of the dura's properties incorporated more fully into the designs, there is potential for improved performance.

Corresponding author: Sean J. Nagel: nagels@ccf.org; Center for Neurological Restoration, Cleveland Clinic Main Campus, Mail Code S31, 9500 Euclid Avenue, Cleveland, OH 44195, USA.

Disclosure statement

Drs. Gillies, Reddy, and Howard may receive patent royalties from the commercial license of the I-Patch intradural stimulator's intellectual properties negotiated by their respective institutions. Drs. Gillies and Howard hold equity in the licensee and serve on its Board of Directors, respectively. Research reported in this publication was supported, in part, by the National Institutes of Health's National Center for Advancing Translational Sciences [Grant Number TL1TR001423]. The content is solely the responsibility of the authors and does not necessarily represent the official views of the National Institutes of Health.

Keywords

Dura mater; spine surgery; electric stimulation; prostheses and implants; biophysical characteristics

1. Introduction

Stephen of Antioch is generally credited with translating the Arabic *alumm al-galidah/jafiyah* or hard mother into the Latin *dura mater* as it is now known [1,2]. The spinal dura mater, mesodermal in origin and arising from the meninx primitive, is a tightly woven, tubular membrane that encases the spinal cord along its length and partitions the central and peripheral nervous system [1]. The steady flow and turnover of cerebrospinal fluid (CSF) within it distends the dura mater until it is compressed against the segmented vertebral scaffold. The spinal cord is suspended within this fluid column that, in turn, shields it from concussive forces and supplies a permissive microenvironment of essential electrolytes and proteins. Even minor perturbations of this space often will have clinical consequences that alert the individual to seek care. For example, the near immediate postural headaches that are frequently reported following a diagnostic lumbar puncture. This early warning system may have evolved to support optimal function of nervous tissue at all times and prevent exposure to pathogens.

As an immunologically privileged site however, the risk is elevated when this membrane is perforated with a needle or splayed open for diagnosis or therapy. Consequently, the delivery of pharmaceutical compounds or the implantation of medical devices through the dura mater involves additional concerns that must be taken into account during the development of such products. This has in no small part limited the number of devices currently Food and Drug Administration (FDA) approved for permanent implant into the intrathecal space to just infusion or drainage catheters. Principal among these concerns are the risk of an unremitting leak of CSF. Therefore, it is important to understand the structural and biomechanical properties of this membrane, the repair mechanisms for it, and the response of the dural tissue to damage. In addition, improved knowledge of the electromagnetic characteristics of the membrane will help drive advances in spinal cord stimulation (SCS) and imaging of the dural sac and its contents. In this review, we discuss the known and, in some cases, unknown biophysical properties of the dura mater that are critical to the design of future medical devices to be employed in this realm of neurosurgery (Table 1). We anticipate that doing so will help prompt subsequent studies and reports that will fill in the gaps in knowledge that exist presently, and hence be useful to those seeking to develop and test novel intradural and intrathecal devices.

2. Biological and structural properties

2.1. Gross anatomical properties

Although dura mater is a continuous membrane that encloses the brain and the spinal cord, the spinal dura mater differs from the cranial dura mater. The external endosteal layer of cranial dura mater ends at the foramen magnum continues as the periosteum of the spinal

canal. Thus, the spinal dura mater is composed of the inner or meningeal layer of cranial dura mater. Caudally, the spinal dura ends at the level of S2 where it becomes a thin cord-like extension (coccygeal ligament or filum terminale) that anchors the dural sac to the sacral periosteum. The dura mater is attached to the circumference of the foramen magnum and the second and third vertebrae. It is also attached anteriorly to the posterior longitudinal ligament by the fibrous Bands of Hofmann. The posterior surface is relatively more mobile and the connective tissue (the meningovertebral ligaments) is less fibrous [3]. Thus, the anterior attachment supports and secures the dura anteriorly in the spinal canal while the posterior surface is allowed greater mobility.

The dural membrane serves not only as a sheath for the spinal cord but also localises and suspends it though the denticulate ligaments that are located between the successive nerve roots. There are also other ligaments and trabeculations in the subdural space that provide additional stability to the spinal cord inside the dural sac. The most notable of these is the fibrous septum posticum [4] which is more fully developed in the upper thoracic spine. The dimensions and morphology of the intrathecal space are different from those of the spinal cord, and vary along the length of the spine (see Figure 1 and “Section 2.4”).

The arterial irrigation of the spinal dura mater comes from the ventral (intraspinal) division of each dorsal spinal artery, with bilateral segmental distribution. In the upper segment, there is anastomosis between the dorsal meningeal arteries and the dural branches of the vertebral, occipital and ascending pharyngeal arteries. The venous drainage is by the extradural venous plexus, with functional valves in the veins at the radicular levels to prevent retrograde flow into the intrathecal extrinsic venous system of the spinal cord [5]. Groen et al. [6] studied the dural innervation and concluded that the dorsal dura has much smaller innervation compared to ventral dura, since the nerves do not reach the medial region in the dorsal side. They further noted that the dorsal nerves are derived from ventral dural plexus, which receives contributions from sinuvertebral nerves, and from the nerve plexus of the posterior longitudinal ligament and the radicular branches of radicular arteries.

2.2. Compositional tissues and microscopic properties

Dura mater is composed largely of fibroblasts, collagen and elastic fibres embedded in an amorphous extracellular ground substance. The collagen provides tensile strength while the elastic fibres provides flexibility and elasticity. The dura has been described as a viscoelastic biological material under normal physiological strains. Although there is some controversy, the collagen fibres are mostly longitudinally oriented. Therefore, the greater tensile strength and stiffness are in the longitudinal direction. Under the microscope, tightly packed collagen fibres are intermixed with elastin fibres. The ratio of collagen to elastin seems to vary along a gradient established by the distance from the CSF with elastin density increasing towards the outer membrane [7]. The collagen is oriented in a cranio-caudal direction.

Studies of the dura mater with electron microscopy have revealed thick collagen fibres arranged in layers and entangled by webs of elastin. For instance, Runza et al. [8], using scanning electron microscopy, showed that the dura mater tissue is formed of parallel overlapping layers and the orientation of these layers changes at different depths. Vandenabeele et al. [9] analysed dura mater specimens via transmission electron

microscopy. They found that the extracellular collagen was helically distributed, wrapping around the spinal axis. Moreover, they reported three distinct layers. First, there was a thin outermost portion with a thickness of 2 mm, with a low density of collagen and elastin fibres and sinuous parallel cell processes, forming a boundary with the epidural space. Second, the middle and thicker portion was richly vascularised and abundant in extracellular collagen intermingled with microfibrils, elastin fibres and some fibroblasts. Lastly, the inner layer, in intimate contact with the parietal arachnoid, presented dark cells ~8 μm thick, with interdigitated cell extensions, enlarged extracellular space, and an absence of a collagen reinforcement— the so-called “dural border cell layer”. The latter demonstrated continuity between the dura and arachnoid layer.

2.3. Surrounding tissues and fluids

While the dura mater outer surface is surrounded by connective tissue in the epidural space, the inner surface is intimately related with the arachnoid membrane which serves as the annular enclosure of the CSF. The epidural space is bounded externally by the osseous wall of the vertebral canal, and layers of loose areolar tissue, fat and a plexus of veins wrap around within it. Metals and metal alloys do not seem to elicit a robust immune reaction in the acute or chronic phase with continual exposure [10]. This is of particular interest to manufacturers of spinal fusion devices.

2.4. Thickness and dural sac morphology

The thickness of the spinal dura mater, the number of fibrous layers and their orientation varies with location along the dural sac [8]. A recent study examined the dura from the craniocervical junction in three cadavers [7]. Multiple sections were measured from each of the cadaver tissue samples. The mean thickness of these sample of dura was $d = (1.106 \pm 0.244)$ mm. In that work, two distinct layers were infrequently observed but this could be related to sampling error. It is likely that the nature of the configurational layering might dependent on the location from which the sample was taken.

In a series of magnetic resonance imaging (MRI)based measurements made on healthy volunteers, Holsheimer et al. [11] found the anterior–posterior (A–P) diameter of the dural sac increased from 13.3 to 16.0 mm over the range of spinal levels C4 to T12. In a larger and more comprehensive study somewhat later, Zaaroor et al. [12] measured the dimensions of the spinal cord, dural sac, and subarachnoid space from C1 through L1. They found that the subarachnoid space was symmetrical on the left and right sides at each transverse level, with an average width of 2.5 mm. However, the posterior and anterior subarachnoid spaces were generally asymmetric and varied in size from 1 to 5 mm. They also found that the ratio of the transverse diameters of the spinal cord and dural sac ranged from 0.44 to 0.72 with a mean value of 0.66, and that the ratio of the respective sagittal diameters ranged from 0.44 to 0.64, with a mean value of 0.56. Lastly, the dimensions of the dural sac were found to vary with those of the vertebral spinal canal along the entire length of the spine.

Lastly, Penning and Wilmink [13] used the myelographic findings obtained from 39 patients to determine how the A–P diameter of the dural sac varied with flexion and extension of the back over the spinal levels L3 to S1. They found, for example, that at L4 the range during

flexion was from 13 to 23 mm with a mean of 17.6 mm, and in extension it varied from 12 to 24 mm with a mean of 18.4 mm. However, they noted that all of their findings were uncorrected for a radiographic enlargement factor of 1.35.

3. Mechanical properties

Mechanical testing has shown roughly 5–11 times greater tensile strength in the longitudinal direction than in the transverse direction of human spinal dura, based on a study of tissues from seven cadavers [14]. The maximum tensile strength found that work was $T_s = 98$ N for samples 1.5 cm long by 1 cm wide). Persson et al. [15] found that the mechanical shear modulus of bovine dura mater remained at roughly $G = 2$ MPa over a 100-fold increase in strain rate (0.01–1.0 s^{-1}), but with the intact dura able to withstand deformations over only a small window before there was irreversible damage. As a point of comparison, Bilston and Thibault [16] found that the elastic modulus of cadaveric spinal cord tissue itself ranged slightly above 1 MPa over similar strain rates. Not unexpectedly, the *in vitro* mechanical properties may not mimic the *in vivo* ones. For example, Zhang et al. [17] compared the *in vivo* Young's modulus of the spinal cord and meninges in the sheep to published results of cadaveric dura and spinal cord measurements using an indentation model that tested the response at displacements of 2–4 mm. They found that the elasticity *in vivo* was much smaller than would be predicted using the cadaveric spinal cord or dura alone. From their measurements, they calculated the Young's modulus to be $Y = (0.022 \pm 0.014)$ MPa, and attributed the difference to the thinness of ovine dura and the transfer of the indentation force from the dura into the underlying CSF.

The *in vivo* preload tension and longitudinal stress are factors that may have clinical relevance when designing implants for the intradural and subdural space. These forces will also predict the size of the opening left after lumbar puncture for device insertion, with further dependence on the orientation of the needle's bevel. A transversely oriented bevel will induce gaping while a longitudinal orientation will tend to seal [14]. The dural layers can be separated, as is sometimes advocated to enlarge the enclosed space in response to increased internal pressure. Layer separation was also done in the past to create a "dural pouch" for what was then referred to as endodural insertion of the electrode arrays of spinal cord stimulators [18]. However, modification of the dura alters its resulting elastoplastic properties [7].

4. Thermal properties

In their comprehensive database of the thermal properties of tissue, which was based on a thorough survey of the literature, McIntosh and Anderson [19] list the following values for dura mater: specific heat capacity, $s = 3364$ J kg^{-1} $°C^{-1}$; thermal conductivity, $k = 0.44$ Wm $^{-1}$ $°C^{-1}$; water content = 68%; density, $\rho = 1174$ kg m^{-3}; blood flow rate = 38 ml min^{-1} $100g^{-1}$; perfusive cooling strength = 28,290 W m^{-3} $°C^{-1}$; and metabolic heat production capacity = 4144 Wm^{-3}. The perfusive cooling strength may be of particular interest in the design of any future intradural medical devices that have active electronic circuitry on board. Recast within that context, for a 1 °C increase in temperature, the dura is capable of perfusively removing ≈28.4 μW of heat from each mm^3 of dural tissue within that zone of

temperature change. For instance, then, a wirelessly powered micro-scale transceiver for monitoring intrathecal pressure could occupy a volume of roughly 4 mm^3 within the dural folds and dissipate roughly 100 μW without raising the local temperature of the dura more than 1 °C.

5. Electromagnetic properties

5.1. Bioelectric characteristics

In early work on the computational modelling of SCS, Sin and Coburn [20] incorporated a parametric representation of the electrical resistivity, ρ_e, of the dura over the range from 60 to 10^4 Ωcm, with the lower value equivalent to that of CSF and the upper value to 2.5 times that of vertebral bone. They concluded that the nominal value of it was approximately ρ_e = 2000 Ωcm = 20 Ωm (which corresponds to an electrical conductivity of $\sigma = 1/\rho_e = 0.05$ S/m), equivalent to the value they chose for epicardial fat. In the modelling work at the University of Twente, Holsheimer employed similar values of conductivity [21], although others [22–24] have more recently used somewhat larger values. Actual measurements of the electrical resistivity of dura mater are very scarce. Those which are reported were made by Oates [25] on *in vitro* samples of feline cerebral dura, with the result that the average resistivity was $\rho_e = (67.4 \pm 26.6)$ Ωcm over the range from 10 to 5 kHz. That result was very near the low end of the range considered originally by Sin and Coburn [20] and roughly 30 times less than the value they adopted. If applicable to human spinal dura mater, those data would imply a conductivity similar to that of CSF, however the lack of any relevant *in vivo* measurements and the significant disagreement between the phenomenological and existing experimental findings make it an open question in need of resolution.

5.2. Biomagnetic characteristics

The biomagnetic characteristics of the body have long been investigated and understood within the context of MR imaging. Schenck's early, thorough review [26] of the role of magnetic susceptibility, χ, in medical imaging provides a wealth of detail on the topic. The values of χ for the various soft tissues are typically taken to be that of water at body temperature, $\chi \approx -9 \times 10^{-6}$, since the available *in vivo* data cluster around that slightly diamagnetic value. As a practical matter, we include dura mater in that category and note that whatever residual susceptibility it has is such that paramagnetic contrast agents must be taken up within it in order for magnetic resonance imaging to resolve certain kinds of localised anomalies in thickness [27,28].

5.3. Optical characteristics

The propagation of optical radiation within a biological tissue is dependent on the wavelength of the source and the absorption coefficient, scattering coefficient and index of refraction of the medium. In order to design laser technologies that can be used safely for diagnostic or therapeutic purposes, it is therefore necessary to characterise the optical properties of the tissue of interest. Early work towards that goal was carried out by Genina et al. [29], who reported indices of refraction for the collagen fibrils and interstitial fluid of dura mater to be $n = 1.474$ and $n = 1.345$, respectively at a wavelength of 589 nm. They went on to show that an aqueous solution of mannitol (0.16 g/ml) will diffuse within the

dura in such a way as to partially match those indices, resulting in a substantial “optical clearing” of the membrane, i.e. a decrease in the level of light scattering within it by factors of 1.5 to 2. Further work in this area [30] has recently shown that the scattering and absorption coefficients of the spinal dura are similar to skeletal muscle which is also composed predominantly of collagen fibres, water and lipids. Their spectrophotometric measurements detected prominent absorption bands at λ = 1450 and λ = 1930 nm, consistent with the water content of the dura, along with more subtle bands associated with its lipid content. Based on the light absorption properties, their work suggests a spectral range of approximately λ = 1900 to 2200 nm as a potentially safe range for medical laser applications in these tissues.

6. Imaging characteristics and approaches

For diagnostic purposes in clinical practice, MR imaging is best for evaluating the spinal dura and surrounding compartments, even though MR may under-estimate the dimensions of the spinal canal compared to CT myelogram [31].

As shown in Figure 1, the dura mater appears as a hypointense thin layer in T_2-weighted MRI. The T_2-weighted images provide better visualisation because of the higher contrast achieved relative to the surrounding structures such as spinal cord, CSF and epidural space. Fat-saturated T_2-weighted MR images can be used to differentiate fluid accumulations from fat pads in the epidural spaces [32].

Advances in other radiological and photo-optical imaging methods have led to improved identification of the dura and enabled minimally invasive surgical approaches to it for several different purposes. Mcleod et al. [33] developed a technique for detecting dural pulsations via real-time ultrasound imaging, with the potential for improved guidance of surgical probes in spine procedures. Ruban et al. [34] reported the management of incidental durotomy with a minimally invasive tubular dilator and microscope. Endoscopic guidance in general has been used in spine surgery for many years in indications such as lumbar stenosis [35], and is capable of visualising the intradural space [36].

In terms of emerging imaging technologies, Giardini et al. [37] have recently shown that optical coherence tomography can be used to image the dura mater and other structures and implants in the lumbar region of a rodent model. Their results demonstrated that with an infra-red (non-ionizing) source operating at a wavelength of 850 nm, resolutions of 80 μm could be achieved, with promising implications for minimally invasive spinal surgery.

7. Surgical procedures

Dural puncture is a routine procedure for diagnostic and therapeutic purposes. Although serious complications including bleeding, infection or even neurological injury are possible, they are quite rare. On the other hand, post-dural puncture headaches are still common even when best practices are followed and in many cases the debate over needle type, bevel orientation and patient position are not settled. A longitudinally oriented needle bevel will tear a flap or slit into the dura whereas a transverse orientation has been shown to leave a

crescent-shaped opening. When longitudinal tension is increased such as with maximal flexion, a larger perforation should be expected [14].

The spinal intradural space is commonly accessed by lumbar dural puncture either for diagnosis, treatment or for anaesthesia purposes. A surgical opening of the dura (durotomy) is also performed by neurosurgeons for treatment of spinal tumours, arachnoid cysts and other pathologies; the dura prior to opening is shown in Figure 2. Unintentional durotomy can occur during spinal surgery and is generally treated intraoperatively, or managed postoperatively with bed rest and a lumbar drain if necessary [38]. Accidental durotomy can also occur after spinal trauma such as vertebral fractures and penetrating wounds. Even spontaneous spinal CSF leak can occur [39]. Given the potential harm of a dural tears and subsequent dural fistula, CSF leaks are a frustrating complication after neurosurgical procedures. Sutures remain the primary means of obtaining satisfactory dural closure.

8. Dural seals

Fibrin sealants can be applied directly to a durotomy suture line, be used to seal suture holes, or fix dural patches. They consist essentially of fibrinogen and thrombin that form a fibrin clot when mixed. These products can be used as a type of liquid glue or as a dry patch, and are safe and beneficial in providing a water-tight closure of the dura [40]. Intraoperative use of one of these products is shown in Figure 3. Epidural blood patch is an effective treatment for dural tears after lumbar puncture resulting in post-dural puncture headache. Using a needle, about 15–20 ml of venous blood is injected slowly into the epidural space near the site of original puncture, with subsequent clotting to patch the CSF leak [41].

Dural substitutes are often needed to expand or replace the dura mater. Many materials have been used as dural substitutes including autografts (e.g. fascia lata and muscle), allograft (e.g. human cadaver skin and lyophilised human dura mater), xenografts (e.g. bovine pericardium) and synthetic polymers. The autologous grafts are preferred, especially because of the low risk of disease transmission and reduced potential for inflammatory and immunologic responses. However, autografts do have disadvantages such as difficulty in achieving a watertight closure, insufficient material to fix large dural defects and, sometimes, the need for an additional incision [42,43]. More recently, absorbable synthetic polymers such as poly (3-hydroxybutyrate-*co*-3-hydroxyvalerate) (PHBV), polyglycolic acid (PGA), poly-L-lactide (PLLA) have attracted attention as biodegradable alternative materials for dural repair. These types of synthetic polymer graft structures might also be used to induce and drive dural regeneration [44].

Polymeric nanofibers, also under study as dural substitutes, offer several advantages over existing artificial repair substrates [45]. The nanofiber scaffold can be coated with various proteins such as glial-derived neurotrophic factors (GDNF) that are slowly released. Early testing has shown that progenitor cells seeded onto the scaffold will differentiate into neurons.

9. Dural instrumentation

9.1. Existing technologies

The premiere examples of medical devices that interact with the dura mater are the access needle, the tools needed for durotomy, the lumbar drain, the intrathecal catheter, and the spinal cord stimulator. Regarding the former, the most familiar type of access cannula is the common Tuohy needle, used universally for dural puncture and subsequent delivery of anaesthetic agents, or for intrathecal access, e.g. during spinal tap. The dynamics of needle insertion into tissues and/or passage through membranes, including dependence on tip geometry, rate of motion, and load distribution during penetration, are generally well-understood [46,47]. Even so, great manual dexterity and physiological acumen are required to avoid inadvertent injury, and especially post-dural puncture headache, and the design of needles and techniques aimed at minimising the risk remains an area of intense study [48–51].

Open intradural exploration (durotomy) remains the standard of care for removing intradural lesions including benign and malignant intramedullary and extramedullary tumours. The dura is opened longitudinally with a scalpel and then reflected with stay sutures. A microscope is routinely used for these operations. The dural tube is reconstituted with running non-absorbable suture and often a dural sealant to minimise CSF leak. However, micro-tears around the suture line are often implicated in CSF fistula formation [52]. Perforating closure devices that are easier to manoeuvre than a needle holder have also been tested [53]. Ideally however, dural closure methods should minimise meningo-neural adhesion common to suture lines or other penetrating wires.

Non-penetrating clips, repurposed from vascular applications, are also now FDA-labeled in USA for dural repair, for example, the AnastoClip® AC Closure System of LeMaitre Vascular Inc., Burlington, MA, USA [54]. They are manufactured in sizes 0.9 to 3.0 mm. These titanium, MRI conditional clips are non-penetrating and are deployed with a rotating steel clip applier intended for small spaces. Kaufman et al. [55] reported no CSF leaks in 26 paediatric patients using this device. Bench testing also supports these findings. Non-penetrating dural clips resisted leakage through polyteterafluoroethylene (ePTFE) sheets (Flex USCI ePTFE sheet, USCI Japan Ltd., Tokyo, Japan) compared to Gore-Tex suture (CV-5, Japan Gore-Tex Inc.). Similar findings were also observed in animal models [52,56]. Dural laceration or clip slip has limited the acceptance of other designs.

Several manufacturers produce and distribute external lumbar drainage catheter systems and lumboperitoneal shunts that are designed to traverse the dura and for placement in the subarachnoid space in order to remove excess CSF. These include, for instance, the Medtronic barium-impregnated silicon catheter (Medtronic, Minneapolis, MN, USA) [57], the Codman Lumbar Drainage Catheter Kit Codman (DePuy Synthes, Raynham, MA, USA) [58], and the Integra Hermetic Lumbar catheters (Integra LifeSciences, Plainsboro, NJ, USA) [59] and OSVII lumbar valve system [60]. There are also several types of catheters used to deliver agents into the intrathecal space, for instance baclofen for the treatment of otherwise intractable spasticity. The designs and modalities of employment for those

devices, as well as the types and severities of the complications that can be associated with them have been discussed in detail recently by Nagel et al. [61].

The dura mater has long played a significant role in the implementation of SCS. At the advent of its use in the late 1960s and early 1970s, most SCS (or “dorsal column stimulation” as it was called then) was carried out with intradural electrode arrays that were anchored to the inner surface of the dura. As mentioned earlier, endodural placement of the electrode array (i.e. within a pouch created by separating layers of the membrane) was also practiced at the time. Gibson-Corley et al. [62] and Nagel et al. [63] surveyed the technologies employed and the clinical results obtained in that era for treatment of chronic pain and spasticity, respectively. Typical of the complications encountered occasionally with those early generation devices were CSF leaks at the passage point of the leads through the dura, infections, spinal cord contusion, intradural haematomas and scar formation. In an effort to circumvent these difficulties, and to reduce the general neurosurgical risks associated with opendura procedures, epidural placement of the stimulator leads came into favour in the mid-1970s. Its clinical acceptance was further augmented by the introduction of minimally invasive percutaneous methods for lead implantation and, at present, all SCS devices and methods are epidural in nature, with rv50,000 SCS cases worldwide each year [64]. These devices are placed in the immediate vicinity of the dorsal dura, thus defining the anatomical spacing between the electrode array and the pial surface of the spinal cord. While this provides a reasonably stable platform for the implanted lead, there is often a compromise in efficacy in that it has long been known that the intervening layer of highly conducting CSF typically limits the depth of stimulation within the spinal cord to a thin outer rim only ≈0.25 mm thick [21]. As discussed below, a new approach to intradural placement of the electrode array seeks to circumvent this.

9.2. Emerging technologies

An example of a novel neuroprosthetic device in which the dura plays a key role is the “I-Patch” spinal cord stimulator [65]. It has undergone several generations of pre-clinical development [66], and is presently at the point where prototypes of it are being designed for eventual pilot studies on patients with spasticity [63]. In their original conception of this device, Howard et al. [67] suggested the possibility of a trans-dural wireless coupling to link an intradural electrode array with an epidural pulse generator in order to enable highly selective stimulation of target sites deep within the spinal cord. They went on to demonstrate the workability of bench top versions of the miniaturised electronics needed for such a trans-dural pairing [68], and also explored *in vivo* wired versions in which the lead bundle traversed the dura via bioresorbable seals [69]. As the latter version promised a faster development track, they then carried out accelerated *in vitro* stress-testing of the leads at the dural seal traversal point and demonstrated robust mechanical and electrical patency of them at $\approx 10^7$ cycles of centimeter-scale reciprocal motion [70]. This well exceeded the lifetime expectations for the possible effects of spinal flexion and extension on that type of implanted device. Anchoring of the extra-dural part of the lead bundle would be achieved in the clinical situation by securing it to a thin titanium strip that bridges the laminectomy gap, with the ends screwed into the opposing vertebral bones, the principle of which was demonstrated in a surgical case involving dural reconstruction following spinal tumour resection [71]. In the

wireless version of the device, the electromagnetic transparency of the dura at the 1.6 MHz carrier frequency was its most important property, while for the wired version of the device, it was the dura's axial tensile strength and ability to meld with dural patch materials to form bioresorbable seals. An early-generation version of the I-Patch is shown in Figure 4. Finite element modelling has demonstrated that direct contact of the electrodes with the pial surface of the spinal cord reduces the electrical shunting effects of the CSF and thus widens the therapeutic window significantly, with the promise of improved selectivity in activating important target fibres within the dorsal columns [72]. The work on this approach is presently ongoing, with additional design concepts for it under consideration.

In a recent review, Wellman et al. [73] have provided a comprehensive survey of the fundamental scientific and engineering principles governing advances in neural implant technology. One of the most critical issues arising in that arena is the mechanical mismatch between the soft tissues of the central nervous system and the stiff materials composing the implants. Minev et al. [74] have addressed this by incorporating stretchable and compliant circuit elements into thin silicone substrates to form a type of "electronic dura mater" that can serve as an interface between the tissues and neuroprostheses. With it, they were able to demonstrate the neuromodulation-induced restoration of ambulation in a rat model of spinal cord injury.

10. Discussion and conclusions

New implantable devices aimed at improving the ability to augment, modify or monitor the central nervous system typically require at least four investigational elements: design and assembly of prototypes, testing of implantation methods, evaluation of device–tissue interactions during *in situ* retainment, and provision for removal. For future development of reliable, safe and durable devices that attach to, or situate on, within or beneath the spinal dura mater, the relevant biophysical properties of that protective membrane must be better elucidated in order to advance from one stage to the next. Any device that jeopardises the protective characteristics of the dura could pose a significant risk of neurological injury or infection. This concern has both nearand long-term relevance that is difficult to predict.

Improvements in miniaturisation have been paralleling the fall in cost to assemble prototypes of new biomedical devices. As a result, the major hurdle that now stands in the way for investigational testing of a potentially viable therapy is no longer technical in nature but rather an insufficient appreciation of the complexity of the space for which the device is intended. In some compartments and organ systems of the body these properties are well-known and fully documented. In others, such as the spinal intradural space, our knowledge is incomplete and the known properties have not been organised in ways useful to biomedical engineers. Therefore, devices modelled to deliver electrical stimulation, sample the microenvironment, or transport fluids or drugs are subject to extensive *in vivo* testing with uncertain and unpredictable results. To help improve this situation, we have reviewed the structural properties of the dura, the related tissues, and the fluid interfaces. Our goal has been to catalogue the relevant mechanical, thermal, and electromagnetic characteristics that have been studied and reported in the literature. We have done this within the context of the existing medical devices and dural repair substitutes now in clinical use and, with an eye

toward future advances in this field, we have also described a novel device intended for intradural deployment. The properties of the dura mater, for instance the thickness of the dural membrane as discussed above and elsewhere [75], constitute important parameters in the design of all such new devices.

Acknowledgements

The authors thank University of Iowa colleague Shawn Roach for assistance with preparation of the figures.

References

[1]. O'Rahilly R, Müller F. The meninges in human development. J Neuropathol Exp Neurol. 1986;45:588–608. [PubMed: 3746345]

[2]. Kothari M, Goel A. Maternalizing the meninges: a pregnant Arabic legacy. Neurol India. 2006;54: 345–346. [PubMed: 17114831]

[3]. Shi BC, Li XM, Li HL, et al. The morphology and clinical significance of the dorsal meningovertebra ligaments in the lumbosacral epidural space. Spine. 2012;18:E1093–E1098.

[4]. Hakky MM, Justaniah AI, David C, et al. The neuroimaging spectrum of septum posticum derangement and associated thoracic myelopathy. J Neuroimaging. 2015;25:818–823. [PubMed: 25907593]

[5]. Becske T, Nelson PK. The vascular anatomy of the vertebro-spinal axis. Neurosurg Clin N Am. 2009;20: 259–264. [PubMed: 19778698]

[6]. Groen GJ, Baljet B, Drukker J. The innervation of the spinal dura mater: anatomy and clinical implications. Acta Neurochir. 1988;92:39–46. [PubMed: 3407473]

[7]. Chauvet D, Carpentier A, Allain J-M, et al. Histological and biomechanical study of dura mater applied to the technique of dura splitting decompression in Chiari type I malformation. Neurosurg Rev. 2010;33: 287–295. [PubMed: 20440557]

[8]. Runza M, Pietrabissa R, Manter S, et al. Lumbar dura mater biomechanics: experimental characterization and scanning electron microscopy observations. Anesth Analg. 1999;88:1317–1321. [PubMed: 10357337]

[9]. Vandenabeele F, Creemers J, Lambrichts I. Ultrastructure of the human spinal arachnoid mater and dura mater. J Anat. 1996;189:417–430. [PubMed: 8886963]

[10]. Rhalmi S, Charette S, Assad M, et al. The spinal cord dura mater reaction to nitinol and titanium allow particles: a 1-year study in rabbits. Eur Spine J. 2007;16: 1063–1072. [PubMed: 17334794]

[11]. Holsheimer J, den Boer JA, Struijk JJ, et al. MR assessment of the normal position of the spinal cord in the spinal canal. AJNR Am J Neuroradiol. 1994;15:951–959. [PubMed: 8059666]

[12]. Zaaroor M, Ko'sa G, Peri-Eran A, et al. Morphological study of the spinal canal content for subarachnoid endoscopy. Minim Invasive Neurosurg. 2006; 49:220–226. [PubMed: 17041833]

[13]. Penning L, Wilmink JT. Biomechanics of lumbosacral dural sac. A study of flexion-extension myelography. Spine. 1981;6:398–407. [PubMed: 7280829]

[14]. Patin DJ, Eckstein EC, Harum K, et al. Anatomic and biomechanical properties of human lumbar dura mater. Anesth Analg. 1993;76:535–540. [PubMed: 8452262]

[15]. Persson C, Evans S, Marsh R, et al. Poisson's ratio and strain rate dependency of the constitutive behavior of spinal dura mater. Ann Biomed Eng. 2010;38:975–983. [PubMed: 20087767]

[16]. Bilston LE, Thibault LE. The mechanical properties of the human cervical spinal cord *in vitro*. Ann Biomed Eng. 1996;24:67–74. [PubMed: 8669719]

[17]. Zhang H, Falkner P, Cai C. In-vivo indentation testing of sheep spinal cord with meninges. Mechan Biolog Syst Mater. 2016;6:99–103.

[18]. Burton C Dorsal column stimulation: optimization of application. Surg Neurol. 1975;4:171–179. [PubMed: 1080904]

[19]. McIntosh RL, Anderson V. A comprehensive tissue properties database provided for the thermal assessment of a human at rest. Biophys Rev Lett. 2010;5:129–151.

[20]. Sin WK, Coburn B. Electrical stimulation of the spinal cord: a further analysis relating to anatomical factors and tissue properties. Med Biol Eng Comput. 1983;21:264–269. [PubMed: 6876898]

[21]. Holsheimer J Computer modelling of spinal cord stimulation and its contribution to therapeutic efficacy. Spinal Cord. 1998;36:531–540. [PubMed: 9713921]

[22]. Lee D, Hershey B, Bradley K, et al. Predicted effects of pulse width programming in spinal cord stimulation: a mathematical modeling study. Med Biol Eng Comput. 2011;49:765–774. [PubMed: 21528381]

[23]. Lempka SF, McIntyre CC, Kilgore KL, et al. Computational analysis of kilohertz frequency spinal cord stimulation for chronic pain management. Anesthesiology. 2015;122:1362–1276. [PubMed: 25822589]

[24]. The Foundation for Research on Information Technologies in Society [Internet]. Database summary of EM and thermal tissue parameters. [cited 2017]. Available from: https://www.itis.ethz.ch/virtual-population/tissue-properties/database/database-summary/

[25]. Oates AD. Cerebral dura mater impedance measurements using a specially designed chamber [master's thesis]. Case Western Reserve University; 5 2000.

[26]. Schenck JF. The role of magnetic susceptibility in magnetic resonance imaging: MRI magnetic compatibility of the first and second kinds. Med Phys. 1996;23:815–850. [PubMed: 8798169]

[27]. Vargas-Bellina V, Saavedra-Pastor H, Alvarado-Rosales M, et al. Idiopathic hypertrophic pachymeningitis: a case report. Rev Neurolog. 2009;48:300–303.

[28]. Pavelek Z, Ryska R, Zizka J, et al. Idiopathic hypertrophic cranial pachymeningitis – two case reports. Ceska a Slovenska Neurologie a Neurochirurgie. 2016; 79:604–607.

[29]. Genina ' EA, Bashkatov AN, Kochubey VI, et al. Optical clearing of human dura mater. Opt Spectrosc. 2005;98:470–476.

[30]. Filatova SA, Shcherbakov IA, Tsvetkov VB. Optical properties of animal tissues in the wavelength range from 350 to 2600 nm. J Biomed Opt. 2017;22:035009.

[31]. Naganawa T, Miyamoto K, Ogura H, et al. Comparison of magnetic resonance imaging and computed tomogram-myelography for evaluation of cross sections of cervical spinal morphology. Spine. 2011;36:50–56. [PubMed: 20581762]

[32]. Watanabe A, Horikoshi T, Uchida M, et al. Diagnostic value of spinal MR imaging in spontaneous intracranial hypotension syndrome. Am J Neuroradiol. 2009; 30:147–151. [PubMed: 18768717]

[33]. McLeod AJ, Baxter JSH, Ameri G, et al. Detection and visualization of dural pulsation for spine needle interventions. Int J Cars. 2015;10:947–958.

[34]. Ruban D, O'Toole JE. Management of incidental durotomy in minimally invasive spine surgery. Neurosurg Focus. 2011;31:E15.

[35]. Khoo LT, Fessler RG. Microendoscopic decompressive laminotomy for the treatment of lumbar stenosis. Neurosurgery. 2002;51:S146–S154. [PubMed: 12234442]

[36]. Warnke JP, Tschabitscher M, Nobles A. Thecaloscopy: the endoscopy of the lumbar subarachnoid space, part I: historical review and own cadaver studies. Minim Invasive Neurosurg. 2001;44:61–64. [PubMed: 11487785]

[37]. Giardini ME, Zippo AG, Valente M, et al. Electrophysiological and anatomical correlates of spinal cord optical coherence tomography. PLoS One. 2016;11:e0152539. [PubMed: 27050096]

[38]. Williams BJ, Sansur TA, Smith JS, et al. Incidence of unintended durotomy in spine surgery based on 108,478 cases. Neurosurgery. 2011;68:117–124. [PubMed: 21150757]

[39]. Schievink WI. Spontaneous spinal cerebrospinal fluid leaks and intracranial hypotension. JAMA. 2006;295: 2286–2296. [PubMed: 16705110]

[40]. Esposito F, Angileri FF, Kruse P, et al. Fibrin sealants in dura sealing: a systematic literature review. PLoS One. 2016;11:e0151533. [PubMed: 27119993]

[41]. van Kooten F, Oedit R, Bakker SLM, et al. Epidural blood patch in post dural puncture headache: a randomized, observer-blind, controlled clinical trial. J Neurol Neurosurg Psychiat. 2008;79:553–558. [PubMed: 17635971]

[42]. Costantino PD, Wolpoe ME, Govindaraj S, et al. Human dural replacement with acellular dermis: clinical results and a review of the literature. Head Neck. 2000;22:765–771. [PubMed: 11084636]

[43]. di Nuzzo G, Luongo M, Parlato C, et al. Cranial reconstruction using bioabsorbable calcified triglyceride bone cement. J Craniofac Surg. 2010;21:1170–1174. [PubMed: 20613599]

[44]. Xie J, MacEwan MR, Ray WZ, et al. Radially aligned, electrospun nanofibers as dural substitutes for wound closure and tissue regeneration applications. ACS Nano. 2010;4:5027–5036. [PubMed: 20695478]

[45]. Mohtaram NK, Ko J, Agbay A, et al. Development of a glial cell-drived neurotrophic factor-releasing artificial dura for neural tissue engineering applications. J Mater Chem B. 2015;3:7974–7985.

[46]. van Gerwen DJ, Dankelman J, van den Dobbelsteen JJ. Needle-tissue interaction forces-a survey of experimental data. Med Eng Phys. 2012;34:665–680. [PubMed: 22621782]

[47]. van de Berg NJ, de Jong TL, van Gerwen DJ, et al. The influence of tip shape on bending force during needle insertion. Sci Rep. 2017;7:40477. [PubMed: 28074939]

[48]. Arevalo-Rodriquez I, Munoz L, Godoy-Casasbuenas N, Ciapponi A, Arevalo JJ, Boogaard S, Roque I, Figuls M. Needle gauge and tip designs for preventing postdural puncture headache (PDPH). Cochr Database Syst Rev. 2017;4:CD010807.

[49]. Xu H, Liu Y, Song WY, et al. Comparison of cutting and pencil-point spinal needle in spinal anesthesia regarding postdural puncture headache. a meta-analysis. Medicine. 2017;96:e6527. [PubMed: 28383416]

[50]. Nath S, Badhiwala JH, Alhazzani W, et al. Atrumatic versus traumatic lumbar puncture needles: a systematic review and meta-analysis protocol. BMJ Open. 2017;7:e014478.

[51]. Chau A, Bibbo C, Huang CC, et al. Dural puncture epidural technique improves labor analgesia quality with fewer side effects compared with epidural and combined spinal epidural techniques a randomized clinical trial. Anesth Analg. 2017;124:560–569. [PubMed: 28067707]

[52]. Ito K, Aoyama T, Horiuchi T, et al. Utility of nonpenetrating titanium clips for dural closure during spinal surgery to prevent postoperative cerebrospinal fluid leakage. J Neurosurg Spine. 2015;23:812–819. [PubMed: 26315957]

[53]. Park P, Leveque J-C, La Marca F, et al. Dural closure using the U-clip in minimally invasive spinal tumor resection. Clin Spine Surg. 2010;23:486–489.

[54]. LeMaitre Vascular [Internet]. Burlington, MA: LeMaitre Vascular, Inc.; 2017 Available from: http://www.lemaitre.com/medical_anastoclip_gc_vessel_closure.asp

[55]. Kaufman BA, Matthews AE, Zwienenberg-Lee M, et al. Spinal dural closure with nonpenetrating titanium clips in pediatric neurosurgery. J Neurosurg Pediatr. 2010;6:359–363. [PubMed: 20887109]

[56]. Faulkner ND, Finn MA, Anderson PA. Hydrostatic comparison of nonpenetrating titanium clips versus conventional suture for repair of spinal durotomies. Spine. 2012;37:E535–E539. [PubMed: 22322376]

[57]. Medtronic [Internet]. Minneapolis, MN: Medtronic; [5 2016]. Available from: http://www.medtronic.com/us-en/healthcare-professionals/products/neurological/critical-care/duet-external-drainage-monitoring-system/edms-catheters.html

[58]. DePuy Synthes [Internet]. Lumbar external drainage system. Raynham, MA: DePuy Synthes; [31 1 2018]. Available from: https://www.depuysynthes.com/hcp/codman-neuro/products/qs/Lumbar-External-Drainage-System

[59]. Integra [Internet]. Limits uncertainty via an easy setup and a secure fixation to the IV pole. Plainsboro, NJ: Integra LifeSciences Holding Corp. 2016 Available from: https://www.integralife.eu/products/neuro/neurocritical-care/evd-system-accudrain/

[60]. Integra [Internet]. Plainsboro, NJ: Integra LifeSciences Holding Corp Available from: https://www.integralife.com/osv-ii-two-piece-shunt-system/product/hydrocephalus-shunts-flow-regulating-valves-osv-ii-valvesosv-ii-two-piece-shunt-system

[61]. Nagel SJ, Reddy CG, Frizon L, et al. Intrathecal therapeutics: device design, access methods and complication mitigation. Neuromodulation. 2017 [9 29]; doi:10.1111/ner.12693

[62]. Gibson-Corley KN, Flouty O, Oya H, et al. Postsurgical pathologies associated with intradural electrical stimulation in the central nervous system: design implications for a new clinical device. BioMed Res Int. 2014; 2014:989175. [PubMed: 24800260]

[63]. Nagel SJ, Wilson S, Johnson MD, et al. Spinal cord stimulation for spasticity: historical approaches, current status,and future directions. Neuromodulation. 2017;20:307–321. [PubMed: 28370802]

[64]. American Association of Neurological Surgeons [Internet]. Spinal cord stimulation. 2018 Rolling Meadows, IL: American Association of Neurological Surgeons Available from: http://www.aans.org/Patients/Neurosurgical-Conditions-and-Treatments/Spinal-Cord-Stimulation

[65]. Flouty O, Oya H, Kawasaki H, et al. A new device concept for directly modulating spinal cord pathways: initial in vivo experimental results. Physiol Meas. 2012;33:2003–2015. [PubMed: 23151433]

[66]. Dalm BD, Viljoen SV, Dahdaleh NS, et al. Revisiting intradural spinal cord stimulation: an introduction to a novel intradural spinal cord stimulation device. Innov Neurosurg. 2014;2:13–20.

[67]. Howard MA III, Utz M, Brennan TJ, et al. Intradural approach to selective stimulation of the spinal canal for treatment of intractable pain: design principles and wireless protocol. J Appl Phys. 2011;110:044702.

[68]. Song S-H, Gillies GT, Howard MA III, et al. Power and signal transmission protocol for a contactless subdural spinal cord stimulation device. Biomed Microdevices. 2013;15:27–36. [PubMed: 22892642]

[69]. Oya H, Safayi S, Jeffery ND, et al. Soft-coupling suspension system for an intradural spinal cord stimulator: biophysical performance characteristics. J Appl Phys. 2013;114:164701.

[70]. Viljoen S, Oya H, Reddy CG, Dalm BD, et al. Apparatus for simulating dynamic interactions between the spinal cord and soft-coupled intradural implants. Rev Sci Instrum. 2013;84:114303. [PubMed: 24289414]

[71]. Dalm BD, Viljoen S, Gillies GT, et al. A novel dural reconstruction method following spinal tumor resection. Neursurg Quart. 2016;26:251–255.

[72]. Huang Q, Oya H, Flouty OE, et al. Comparison of spinal cord stimulation profiles from intraand extradural electrode arrangements by finite element modeling. Med Biol Eng Comput. 2014;52:531–538. [PubMed: 24771203]

[73]. Wellman SM, Eles JR, Ludwig KA, et al. A materials roadmap to functional neural interface design. Adv Funct Mater. 2017;1701269. [PubMed: 29805350]

[74]. Minev IR, Musienko P, Hirsch A, et al. Biomaterials. Electronic dura mater for long-term multimodal neural interfaces. Science. 2015;347:159–163. [PubMed: 25574019]

[75]. Hong J-Y, Suh S-W, Park S-Y, et al. Analysis of dural sac thickness in human spine-cadaver study with confocal infrared laser microscope. Spine J. 2011;11: 1121–1127. [PubMed: 22172494]

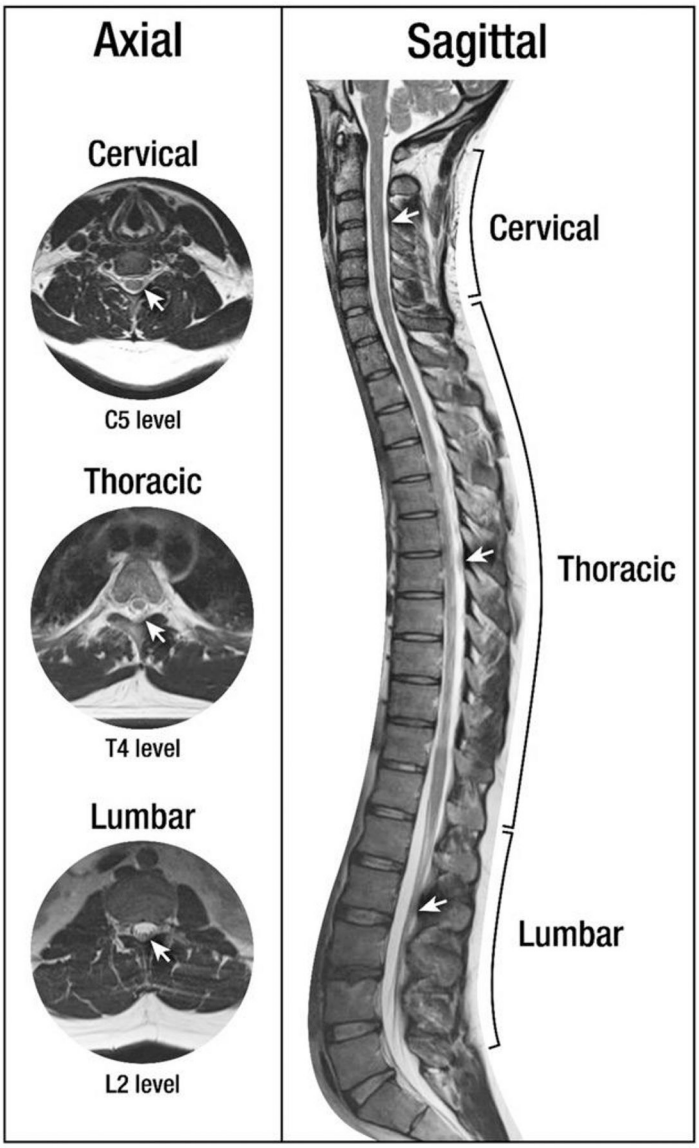

Figure 1.
Axial and sagittal T2-MRI images of spinal anatomy. White arrows denote the dura mater.

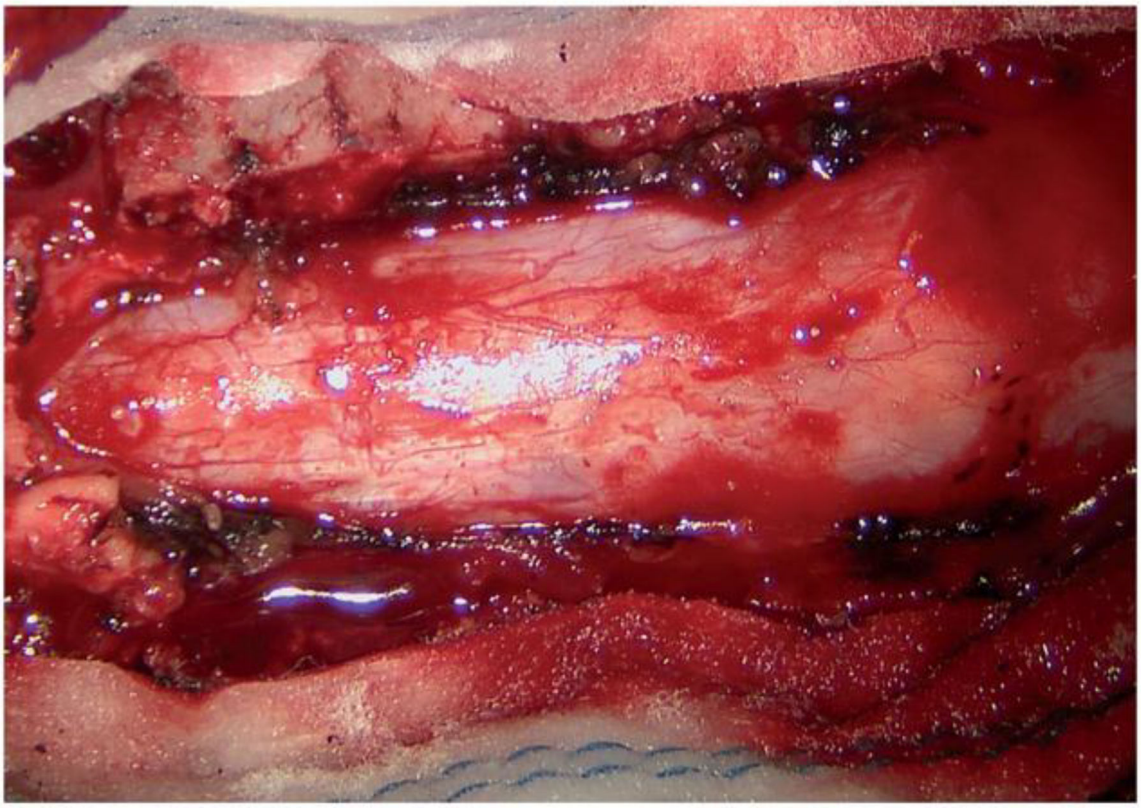

Figure 2.
Intraoperative view of the dura mater as accessed for durotomy.

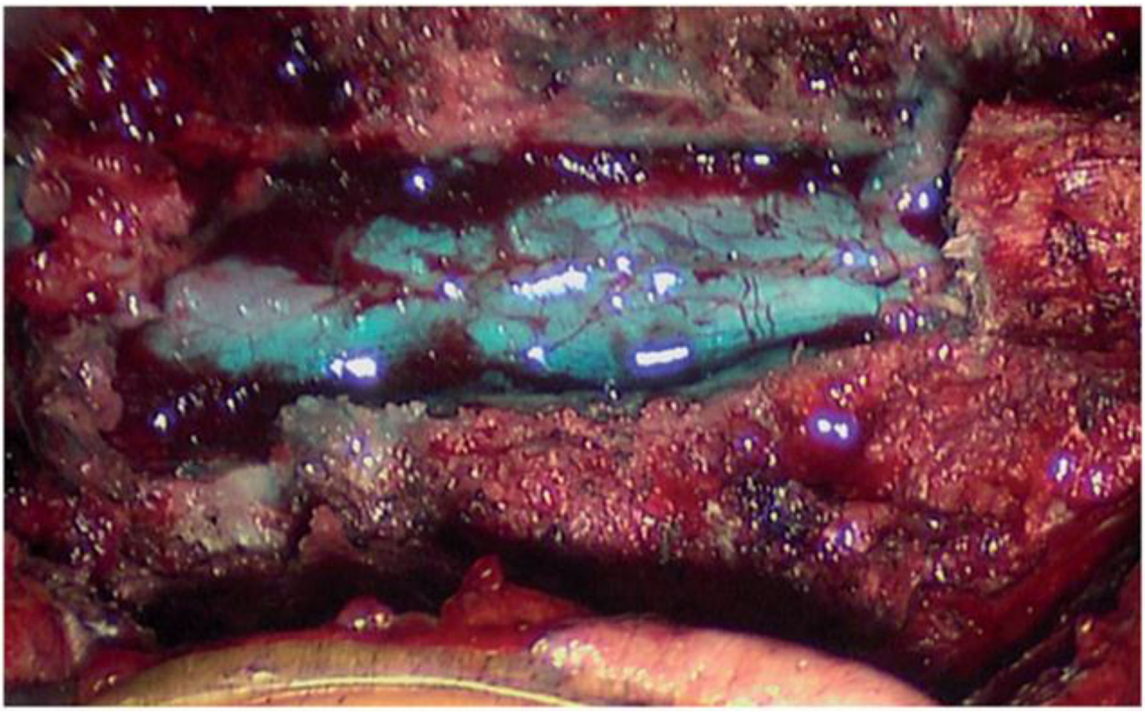

Figure 3.
Intraoperative view of a dural sealant used after primary dural closure.

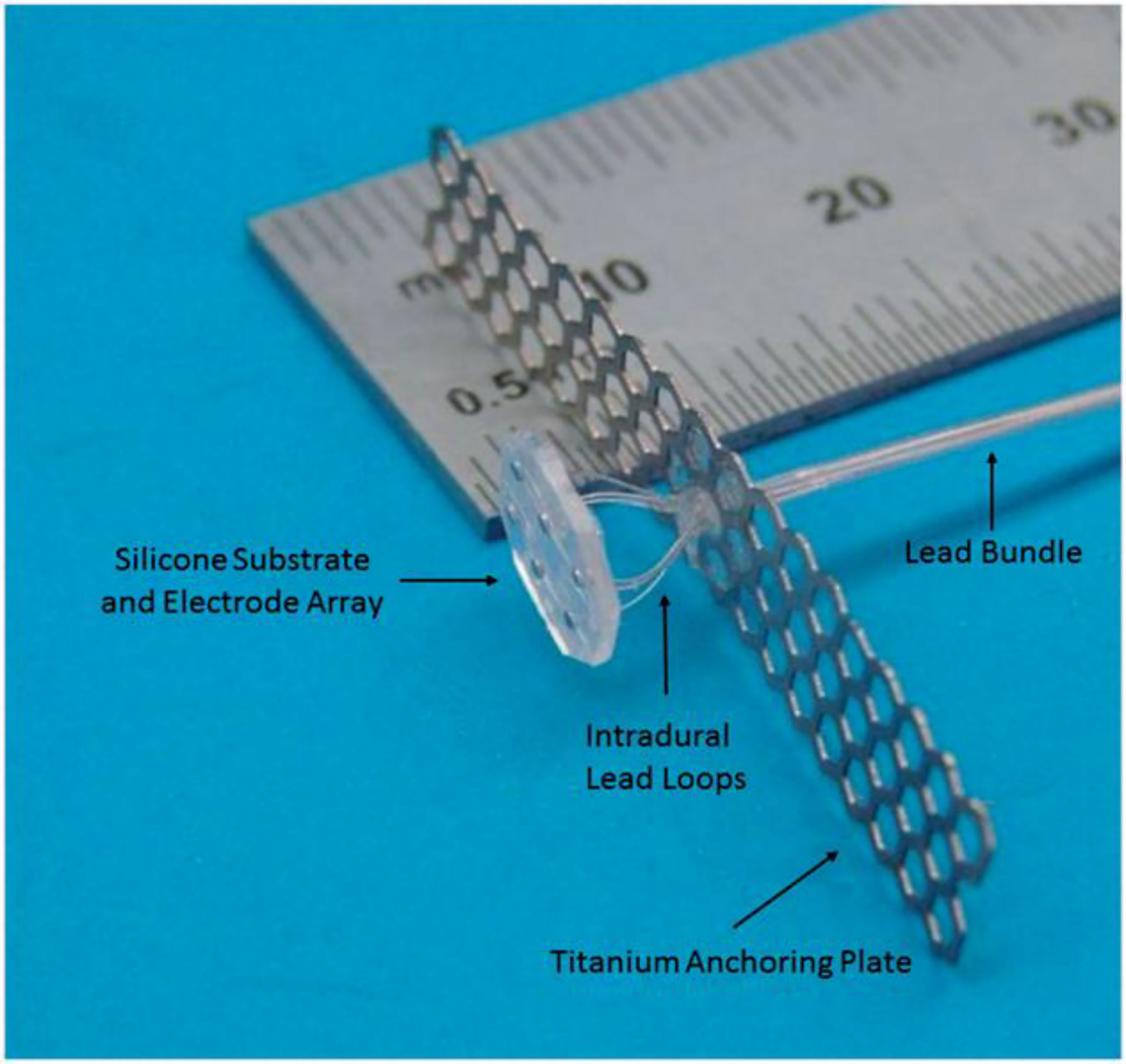

Figure 4.
Early-generation version of the I-Patch intradural spinal cord stimulator. The smallest division of the lower scale of the ruler is 0.5 mm. Dural sealant material not shown.

Table 1.

Biophysical properties of the spinal dura mater.

Author	Year	Property	Method of measurement	Results	Comments
Sin and Coburn [20]	1983	Electrical resistivity (phenomenological)	Computational modeling	ρ_e = 20 Ωm = σ.1/ρ_e = 0.05 S/m	Same value as that specified for epicardial fat
Groen et al. [6]	1988	Innervation	Anatomical study	Dorsal dura is much less innervated compared to ventral dura	Dorsal nerves derived from the ventral dural plexus
Patin et al. [14]	1993	Tensile strength	Instron biomechanical testing	Maximum was T_S = 98 N for samples 1.5 cm long by 1.0 cm wide	Longitudinal tensile strength 5 to 11 times greater the that of the transverse direction
Vandenabeele et al. [9]	1996	Microscopic structure	Transmission electron microscopy	**1** Outermost portion with a thickness of 2 μm, with a low density of collagen **2** Middle and thicker portion was richly vascularized and abundant in extracellular collagen intermingled **3** Inner layer, in intimate contact with the parietal arachnoid, presented dark cells ~8 mm thick, with interdigitated cell extensions, enlarged extracellular space	Helically distributed extracelluar collagen
Schenck [26]	1996	Magnetic susceptibility	Standard value accepted for soft tissues	$\chi \approx -9 \times 10^{-6}$	Taken to be that of water at body temperature
Runza et al. [8]	1999	Microscopic structure, tensile strength, stiffness	Scanning electron microscopy and monoxial tensile tests	Close correlation between the microstructural anatomy and biomechanical properties of lumbar dura mater	Stronger tensile strength and stiffness in the longitudinal direction
Oates [25]	2000	Electrical resistivity (measured)	Impedance determined from voltage produced across a sample of dura mater through which constant amplitude currents were driven	Average resistivity: ρ_e = (67.4 ± 26.6) Ωcm	Frequency range: 10 Hz to 5 kHz
Genina et al. [29]	2005	Optical characteristics	Diffusion of aqueous mannitol to produce matching of indices of refraction	n =1.474 (dural collagen fibrils) and n = 1.345 (dural interstitial fluid) at λ 589 nm	The manitol infusion produced “optical clearing” of the membrane
Chauvet et al. [7]	2009	Thickness	Optical microscopy/digital micrometer gauge	Mean: d = (1.106 ± 0.244) mm	Craniocervical junction specimens
Watanabe et al. [32]	2009	MR imaging characteristics	Spinal MR imaging	Hypointense thin layer in $T_1$and T_2-weighted MRI	The T_2-weighted images provide better visualization because of the higher contrast achieved relative to the surrounding structures
McIntosh and Anderson [19]	2010	Thermal characteristics	Literature review	Heat capacity: s = 3364 J kg^{-1} °C^{-1} Thermal conductivity: k = 0.44 W m^{-1} °C^{-1} Water content = 68% Density: ρ = 1174 kg m^{-3} Blood flow	Based in literature review the authors developed a database of thermal properties for 43 human tissues

Author	Year	Property	Method of measurement	Results	Comments
				rate = 38 ml min^{-1} 100 g^{-1} Perfusive cooling strength = 28390 W m^{-3} $°C^{-1}$ Metabolic heat production = 4144 W m^{-3}	